UNIVERSITY OF MICHIGAN

engineering
RESEARCH
institute

REPORT NO. 2

MECHANISM OF NON-VISCOUS FLOW THROUGH SWIRL-CHAMBER NOZZLES

Project 2041-2

by

J. LOUIS YORK
M. R. TEK
H. E. STUBBS
T. E. SLYKHOUSE

JUNE, 1953

U. S. NAVY DEPARTMENT
CONTRACT N123s-80065, TASK ORDER NO. 2

ENGINEERING RESEARCH INSTITUTE
University of Michigan
Ann Arbor

MECHANISM OF NON-VISCOUS FLOW THROUGH SWIRL-CHAMBER NOZZLES

J. Louis York

Associate Professor of Chemical and Metallurgical Engineering

M. R. Tek

Research Assistant in Engineering Research Institute

H. E. Stubbs

Research Associate in Engineering Research Institute

T. E. Slykhouse

Assistant in Research in Engineering Research Institute

University of Michigan

REPORT NO. 2, PROJECT 2041-2
U. S. NAVY DEPARTMENT
CONTRACT N123s-80065, TASK ORDER NO. 2

June 1953

FOREWORD

The work carried out under Task Order No. 2 of Contract N 123s-80065 has been only a part of the entire research effort by the group at the University of Michigan working on sprays and spray nozzles. Additional work has been conducted for other sponsors, and frequently this work is of vital interest to all sponsors and also is of assistance in other projects. This report is on such work, actually performed for the U. S. Air Force, Wright Air Development Center, and reported to them in January 1953. It is included here as one of the reports to the sponsor because it fits the program and leads directly to Report No. 3, "The Mechanism of Viscous Flow Inside Swirl-Chamber Nozzles," (June 1953, J. L. York and T. E. Slykhouse).

This report develops relations for flow of non-viscous fluids and leads to predictions and correlations of nozzle performance. It is substantiated in part by experimental data on water, and it agrees with material published in several different languages and generally unavailable in this country.

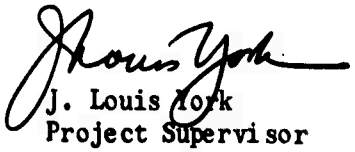

J. Louis York
Project Supervisor
Associate Professor of
Chemical and Metallurgical Engineering

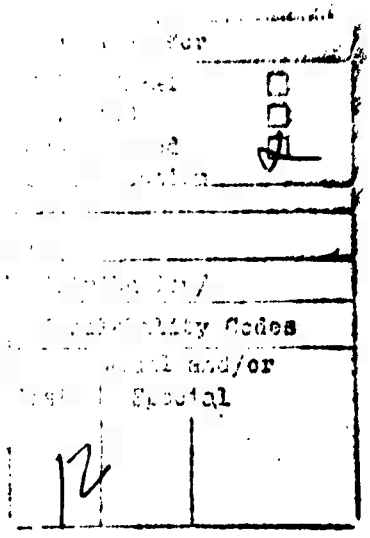

ENGINEERING RESEARCH INSTITUTE
University of Michigan
Ann Arbor

MECHANISM OF NON-VISCOUS FLOW THROUGH SWIRL-CHAMBER NOZZLES

J. Louis York

Associate Professor of Chemical and Metallurgical Engineering

M. R. Tek

Research Assistant in Engineering Research Institute

H. E. Stubbs

Research Associate in Engineering Research Institute

T. E. Slykhouse

Assistant in Research in Engineering Research Institute

June 1953

TABLE OF CONTENTS

LIST OF FIGURES

ABSTRACT

The mechanism of flow in a swirl-chamber spray nozzle is analyzed mathematically, assuming frictionless flow. The resulting equations predict the magnitude of the central air core in such nozzles as a function of the geometry of the nozzle. They also indicate the effect of varying such geometry and predict flow relationships, discharge coefficients, and cone angles.

These mathematical relations are checked experimentally with water in various nozzles, and found to be valid.

NOMENCLATURE

A_s = total cross-sectional area of the entrance slots normal to the tangential velocity component

C = P_i/Q^2

C_o = discharge coefficient

Q = total volume flow rate

V = absolute velocity of the fluid at a given point

g = acceleration of gravity

h = height of the swirl chamber

P_i = pressure above atmosphere in the feed chamber just outside the swirl chamber

P_r = pressure above atmosphere at the point corresponding to radius "r"

r = radius of any point in the streamline used as an example

r_f = radius of the free surface inside the swirl chamber

r_o = radius of the orifice

r_s = slot radial distance (from axis of symmetry to center of entrance slot opening

U_A = axial velocity

U_R = radial velocity

U_T = tangential velocity

$(U_A)_o$ = axial component of velocity at exit orifice

$(U_T)_o$ = tangential component of velocity at exit orifice

$(U_T)_s$ = tangential component of velocity through entrance slots

α = cone angle degrees

η = air core-orifice ratio

ρ = mass density of the liquid

MECHANISM OF NON-VISCOUS FLOW THROUGH SWIRL-CHAMBER NOZZLES

Studies of drop sizes and distribution in sprays provide information on the results of disintegration of a liquid mass, but control of this disintegration cannot be accomplished without knowledge of all factors leading to the break-up. We have presented information (1) on the mechanism of disintegration of liquid sheets, with special reference to the sheets formed by swirl-chamber spray nozzles. Carrying the investigation one step further, we have examined the mechanism by which the sheet is formed in the nozzle.

The instability of the liquid sheet produced by emerging from the nozzle depends in part on two variables, sheet thickness and velocity, which are influenced strongly by nozzle design. Thus, application of the instability relationships is possible only if these two variables can be evaluated for all points in the conical liquid sheet. An equally important goal of our study was a knowledge of the effect of changes in nozzle geometry and operation on the behavior of the liquid flowing through the nozzle. An analysis of the flow in a swirl-chamber nozzle is therefore the first step in gaining an understanding of the mechanism by which the sheet is formed.

Analysis

Figure 1 is a diagram of the main design features of a swirl-chamber nozzle. The nozzle consists of a round chamber into which fluid is forced through tangential slots. The fluid is discharged through a central orifice of smaller radius than that of the circle at which the

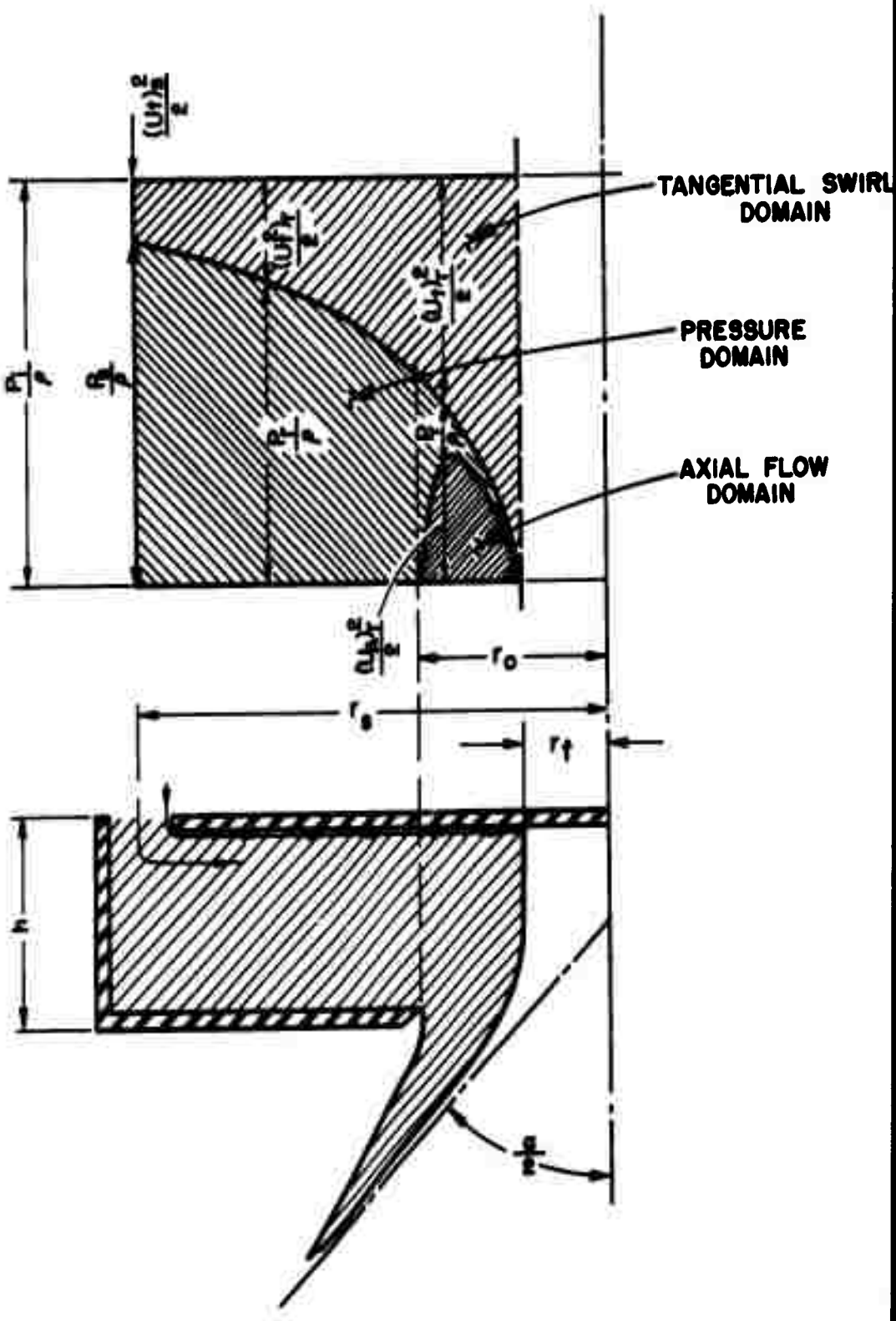

Figure 1. Basic Diagram of a Swirl-Chamber Nozzle.

slots enter. The tangential velocity therefore increases during the passage of the fluid through the swirl chamber.

The pressure energy decreases gradually along each streamline by conversion to tangential, radial, and axial velocity components. When the liquid reaches the orifice of the swirl nozzle, only kinetic energies of axial and tangential motion are present. Concentric with the axis of the chamber is an air core in which the pressure is atmospheric. The liquid emerges in the form of an annulus which curves out into a nearly conical form after leaving the orifice, and subsequently breaks up into drops.

A mathematical analysis of the behavior of the liquid flowing through the nozzle is based primarily upon a detailed study of the energy conversions occurring within the nozzle. This study is greatly simplified by assuming the liquid to be frictionless and incompressible. Actually, we need assume only that the energy and momentum losses are quite small compared to the absolute values.

Comparisons of predictions and experimental data show that this assumption is valid for fluids with viscosities of the order of water.

The basic equation for the energy-conversion relationship was proposed by Bernoulli (2):

$$\frac{P_1}{\rho} + \frac{V_1^2}{2} + g z_1 = \frac{P_2}{\rho} + \frac{V_2^2}{2} + g z_2 \qquad (1)$$

where the subscripts $_1$ and $_2$ refer to upstream and downstream points respectively.

Equation 1 may be applied to the particular streamline close to the back plate, between a point in the feed chamber just outside the swirl chamber (upstream point 1) and any point in the streamline (downstream

point 2). Figure 1 shows the geometric relations of the nozzle and the streamline. The pressure just outside the swirl chamber is denoted by p_i and the pressure at any point in the streamline by p_r. The distance of that point from the axis of symmetry is denoted by r. Since $z_1 = z_2$ the Bernoulli equation is

$$p_r = p_i - \frac{\rho}{2}\left(V_r^2 - V_i^2\right) \qquad (2)$$

In general, $V_i \cong 0$ and

$$V_r^2 = u_T^2 + u_R^2 + u_A^2 \qquad (3)$$

For the streamline near the back wall of the swirl chamber, $u_A = 0$. The total flow rate, Q, fixes the radial velocity, $u_R = \frac{Q}{2\pi r h}$. In general, it is possible to neglect the radial velocity when compared to the tangential velocity. Equation 3 then shows that $V_r^2 = u_T^2$.

Data from a typical run on an ordinary nozzle will show the magnitude of the relative error resulting from this neglect of u_R. For a flow rate of 66.3 pounds of water per hour through entry slots with a total cross-sectional area of 0.0353 sq. cm., the entrance velocity is 236 cm/sec. The calculated radial velocity is 8.5 cm/sec., corresponding to an error of 3.6 percent if it is neglected. Any increase in the height of the swirl chamber will further reduce the error.

By the principle of conservation of angular momentum:

$$u_T r = (u_T)_s r_s \quad \text{and} \quad u_T = \left(\frac{r_s}{r}\right)(u_T)_s \qquad (4)$$

Other streamlines through the swirl chamber will also have $u_A = 0$ from $r = r_s$ to $r = r_o$. From r_o to r_f an axial component is developed by conversion from pressure, resulting in an energy distribution as shown in Figure 1.

By applying Bernoulli's equation between a point in the inlet chamber just outside the swirl chamber (upstream point 1) and a point in the plane of the exit orifice of the nozzle (downstream point 2), then

$$p_i = p_0 - \frac{\rho}{2}\left(V_i^2 - V_0^2\right) \tag{5}$$

As before, $V_i \cong 0$, and

$$V_0^2 = (u_T)_0^2 + (u_A)_0^2 \tag{6}$$

At the exit orifice, $p_0 = c$, therefore equation 5 becomes

$$p_i = \frac{\rho}{2}\left[(u_T)_0^2 + (u_A)_0^2\right] \tag{7}$$

From Figure 1, we see that

$$(u_A)_0 = \frac{Q}{\pi(r_0^2 - r_f^2)} \tag{8}$$

and from equation 4:

$$(u_T)_0 = \frac{r_s (u_T)_s}{\left(\frac{r_0 + r_f}{2}\right)} \tag{9}$$

Since $(u_T)_s = \frac{Q}{A_s}$, then

$$(u_T)_0 = \frac{2 r_s Q}{A_s (r_0 + r_f)} \tag{10}$$

Substituting equations 8 and 10 into equation 7:

$$p_i = \frac{\rho}{2}\left[\frac{4 r_s^2 Q^2}{A_s^2 (r_0 + r_f)^2} + \frac{Q^2}{\pi^2 (r_0^2 - r_f^2)^2}\right] \tag{11}$$

The dimensionless ratio, $\eta = r_f / r_0$, is significant in this problem and represents the relative size of the air core and the orifice. Introducing it into equation 11 gives

$$p_i = \frac{\rho}{2}\left[\frac{4 r_s^2 Q^2}{A_s^2 r_0^2 (1 + \eta)^2} + \frac{Q^2}{r_0^4 \pi^2 (1 - \eta^2)^2}\right] \tag{12}$$

Substituting equations 4 and 12 into equation 2:

$$p_r = \frac{\rho}{2}\left[\frac{4r_s^2 Q^2}{A_s^2 r_0^2 (1+\eta)^2} + \frac{Q^2}{\pi^2 r_0^4 (1-\eta^2)^2} - \frac{r_s^2 Q^2}{r^2 A_s^2}\right] \qquad (13)$$

When $r = r_f = r_0\eta$, then $p_r = 0$ and

$$\frac{4r_s^2 Q^2}{A_s^2 r_0^2 (1+\eta)^2} + \frac{Q^2}{\pi^2 r_0^4 (1-\eta^2)^2} - \frac{r_s^2 Q^2}{r_0^2 \eta^2 A_s^2} = 0 \qquad (14)$$

Algebraic simplification of equation 14 gives

$$3\eta^4 - 8\eta^3 + \left[6 + \frac{A_s^2}{\pi^2 r_s^2 r_0^2}\right]\eta^2 - 1 = 0 \qquad (15)$$

Equation 15 shows that for a given swirl-chamber nozzle the initial thickness of the liquid sheet issuing from the orifice is constant and independent of the flow rate. It is calculable from nothing more than the geometric design of the nozzle, and depends upon a dimensionless group $(A_s/\pi r_s r_0)$ including the total cross-sectional area of the inlet slots normal to the tangential velocity component, the slot radial distance, and the radius of the orifice. Figure 2 shows η as a function of the nozzle constant $(A_s/\pi r_s r_0)$.

Observation of equation 15 and Figure 2 shows that as the nozzle constant becomes small enough for its square to be negligible compared to 6, then $\eta = 1$, indicating no flow through the nozzle. Predictions of the sheet thickness are less and less reliable as this condition is approached. In practice, nozzle constants below 0.2 give unreliable values for the air-core.

This trend is shown by a simple experiment performed on a transparent plastic nozzle in the laboratory. With four entrance slots into the swirl chamber the predicted value of η was 0.85 and the measured value was 0.687. The addition of four more slots reduced the predicted value to 0.740, which was checked exactly by measurement.

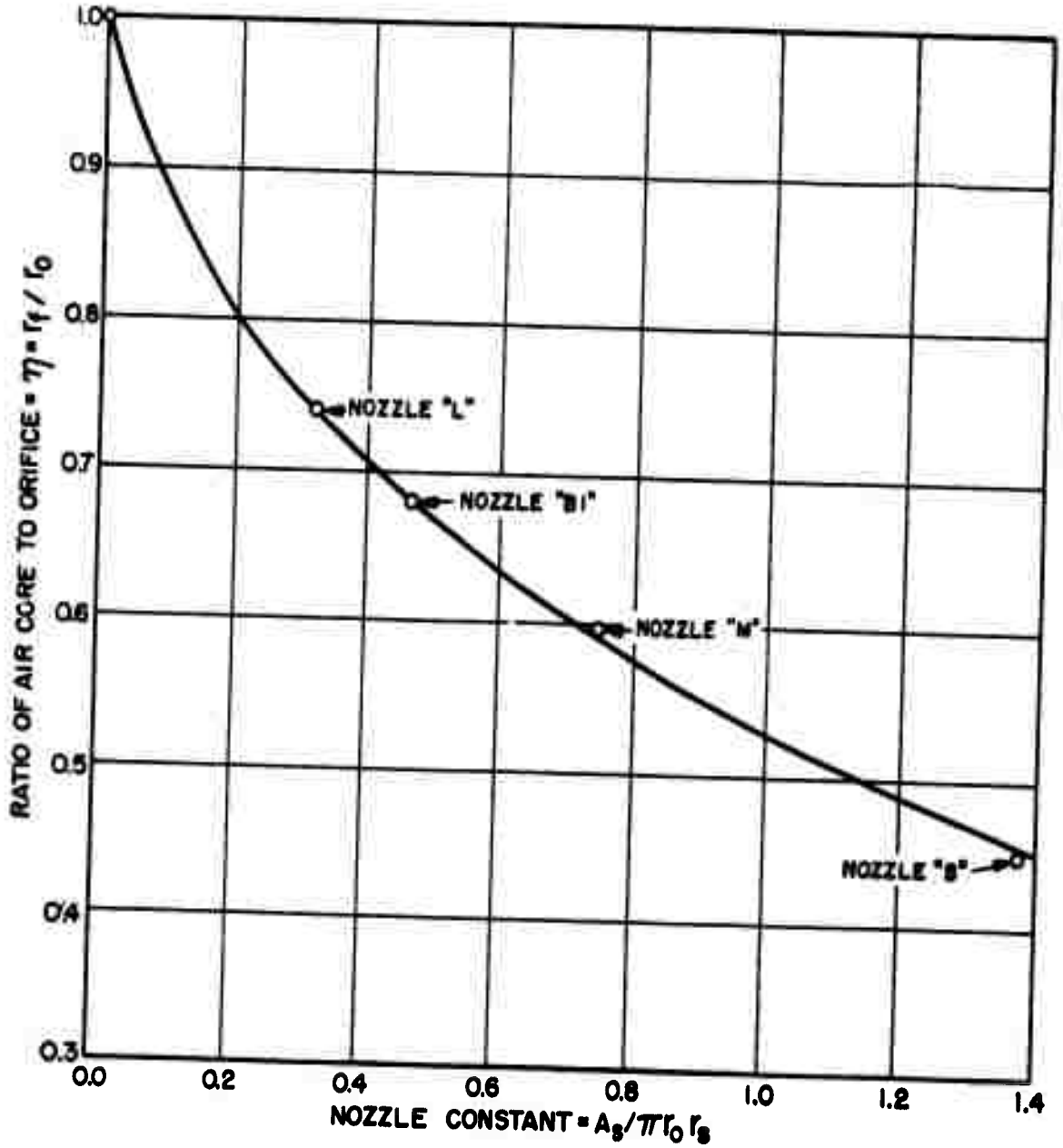

Figure 2. Dependence of Air Core on Nozzle Constant.

Experimental Work

Photographs of 1-microsecond exposure permit measurement of the radius of the free surface. Figure 3 is a silhouette photograph of a transparent plastic nozzle, and Figure 4 is looking into a metal nozzle ("M"), using reflected light. Table I shows a comparison of measurements with the prediction for nozzle "M". The measurements are consistently high, perhaps because the reflected light shows no sharp edge of definition for the air core, but they show no dependence upon flow rate.

TABLE I

COMPARISON OF MEASURED RADII OF FREE SURFACE WITH PREDICTION

NOZZLE "M"

$r_o = 0.0635$ cm, $r_s = 0.246$ cm, $A_s = 0.0356$ sq. cm.

Flow Rate lbs water/ hr.	η, Measured (r_f/r_o)	η, Predicted (r_f/r_o)
100	0.673	0.595
150	0.715	0.595
200	0.712	0.595
250	0.696	0.595
300	0.674	0.595
350	0.620	0.595

Figure 3 is a silhouette photograph of nozzle "L" from the side, showing the air core with a relatively constant radius. The irregular bright streak down the center results from the lensing action of the cylindrical surface on the light through the sides of the air core.

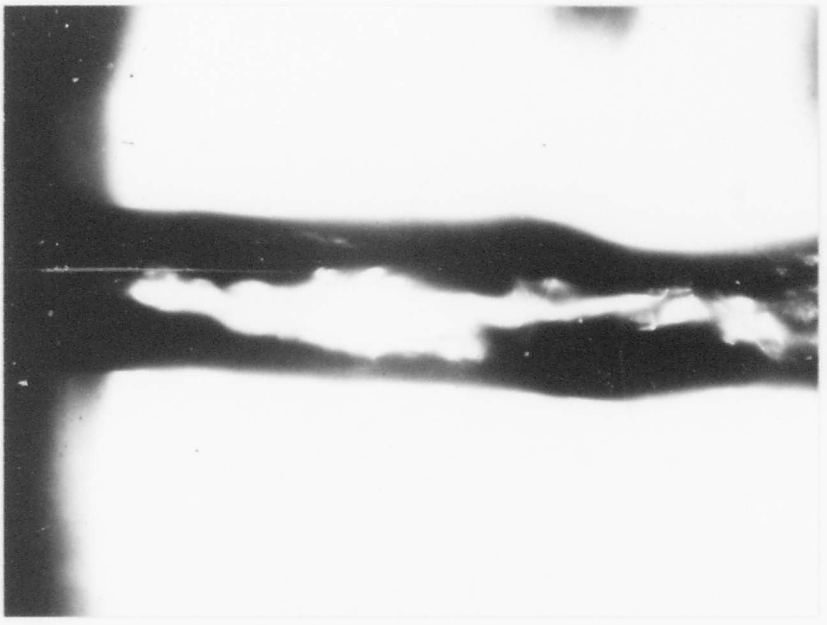

Figure 3. Silhouette of Flow in Transparent Nozzle

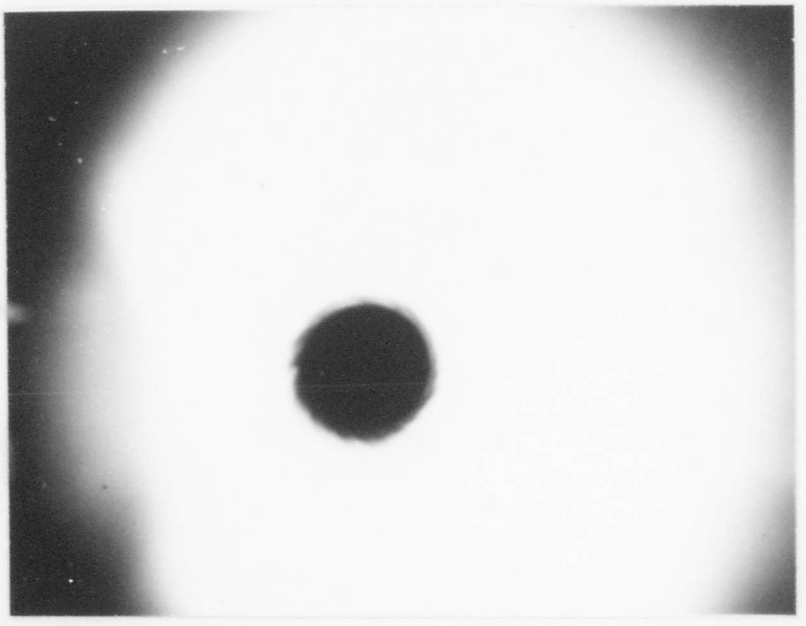

Figure 4. Looking Into a Swirl Nozzle

A hole was drilled in the back plate of one of the plastic nozzles, the diameter being slightly smaller than the predicted air core. No change was observed in the nozzle performance when the hole was opened and closed. Observations of the surface of the air core showed high tangential velocities, which partially supports the assumption of potential flow.

The introduction of a pressurized air stream through the hole in the back plate changed the stability of the surface, as expected. The instability was much greater and the drop size was much smaller. No detailed studies are reported on this effect.

A plastic nozzle with identical orifices in the front and back plates operated with two swirling sprays in each direction and an almost perfect cylindrical air core in the chamber. No detailed studies are reported on this nozzle.

Flow Rates

Equation 12 for a given fluid flowing through a given nozzle is of the form $P = CQ^2$. The coefficient C can be calculated from the geometry and the fluid density, enabling prediction of the pressure-flow relationship. Figure 5 shows a comparison of the prediction with experimental data on five different nozzles.

Variation in Nozzle Design

The effect of altering nozzle design can also be shown from equation 12. The flow rates resulting from a given pressure for the same nozzle with various radii of the orifice are shown in Figure 6. Similarly, the flow rates resulting from a given pressure for the same nozzle with various diameters of the entrance ports (various total slot areas) are shown in Figure 7.

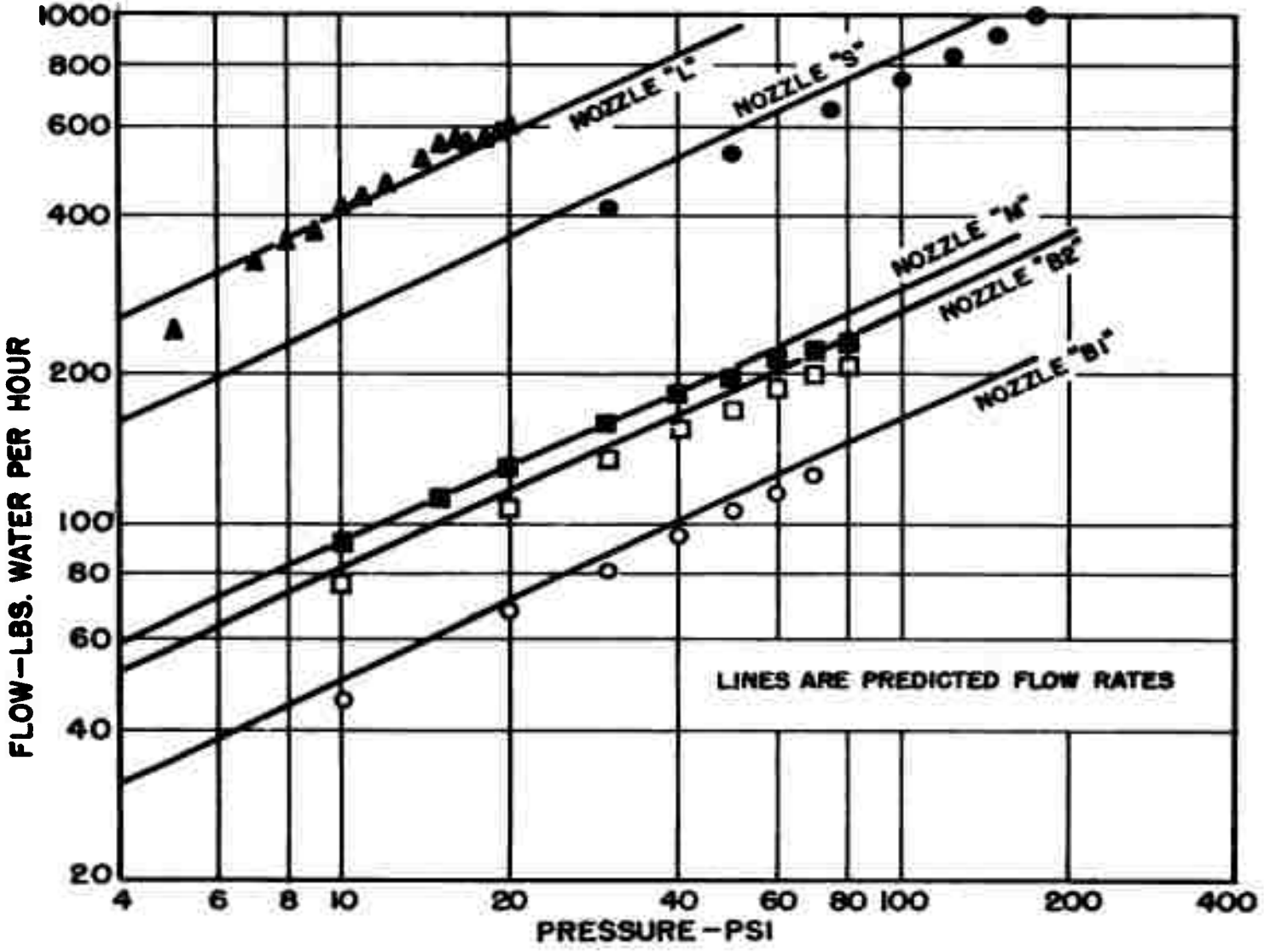

Figure 5. Comparison of Predicted and Measured Flow Rates.

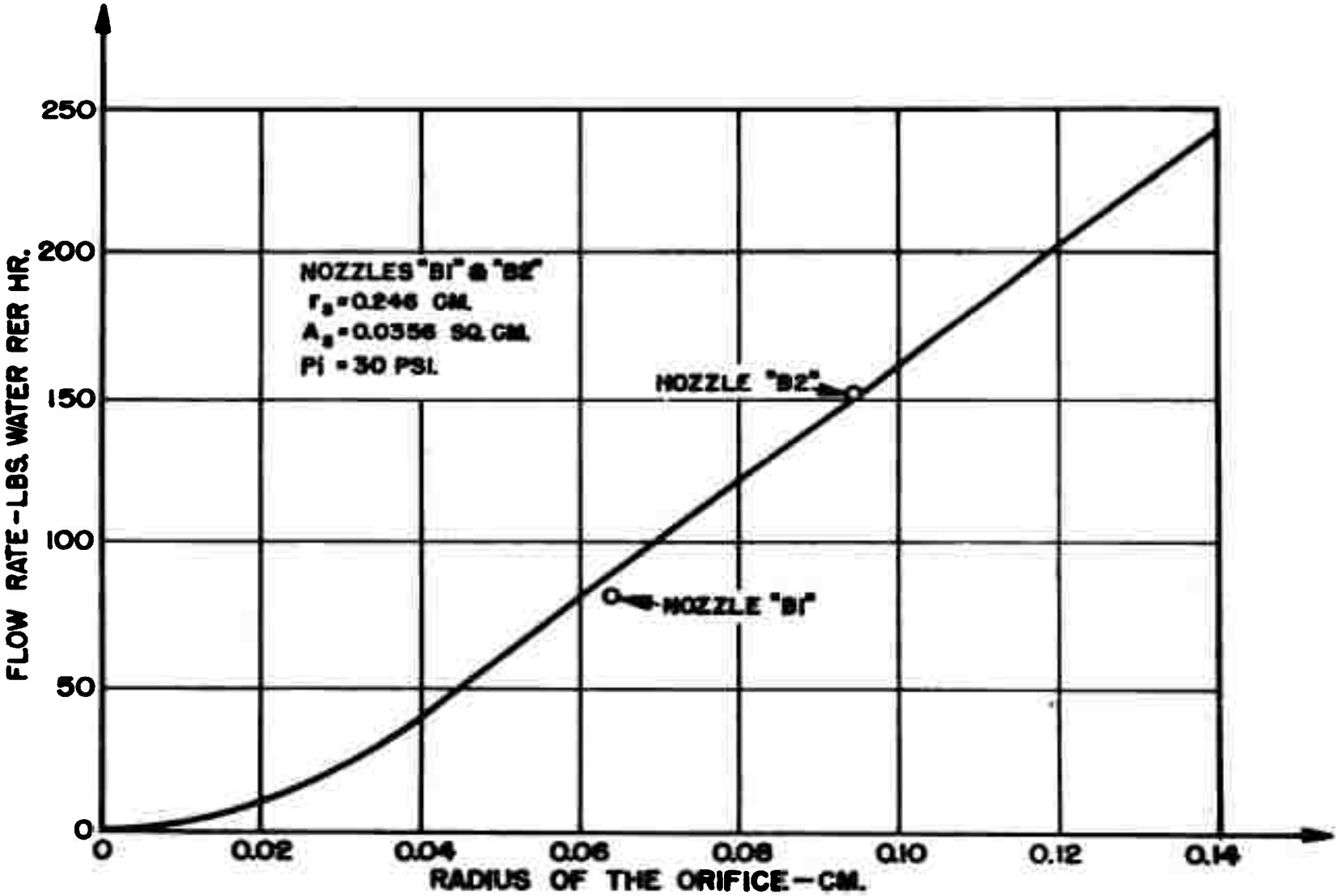

Figure 6. Effect of Orifice Radius on Flow Rate.

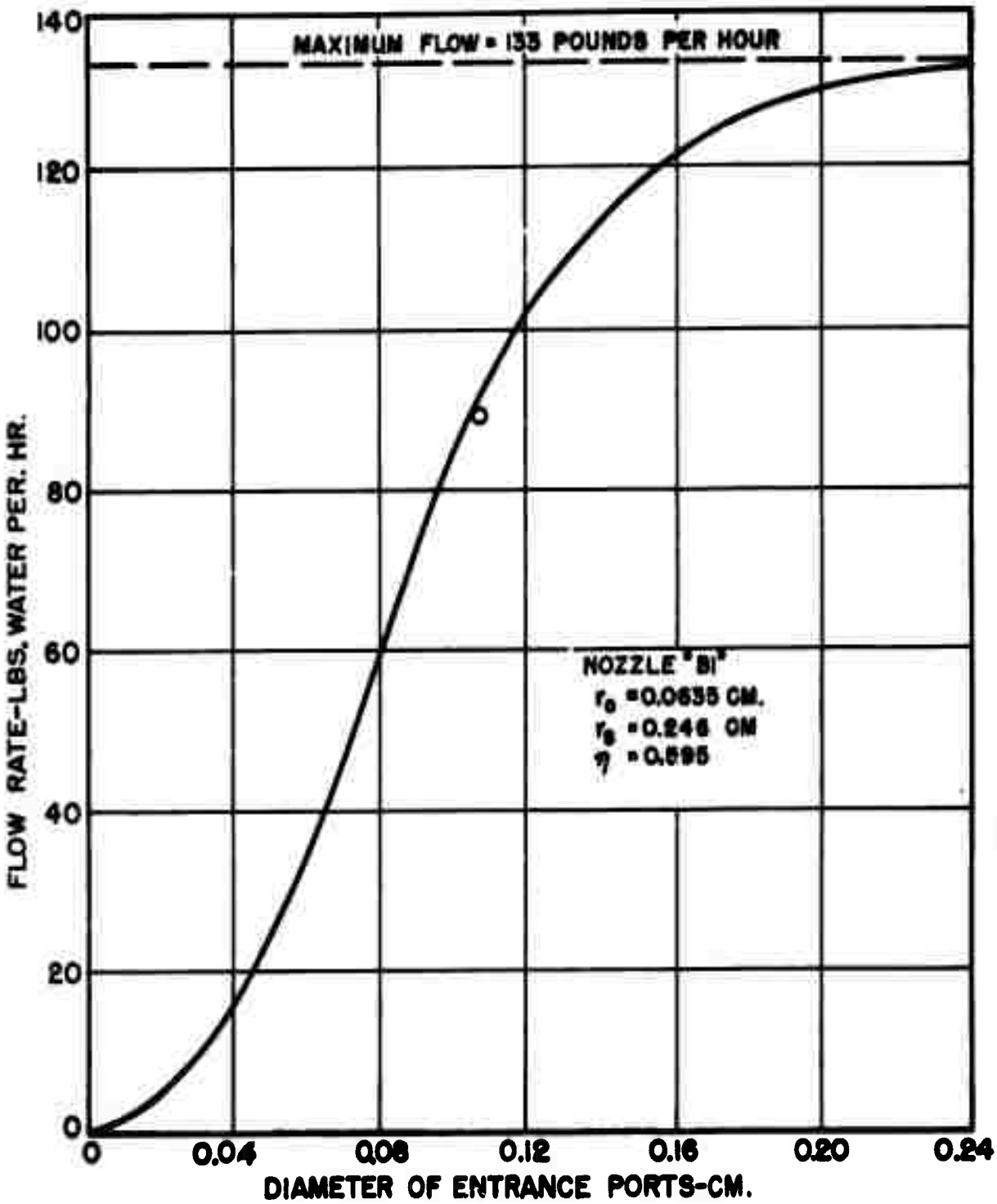

Figure 7. Effect of Entrance-port Area on Flow Rate

Discharge Coefficient

The usual definition of an orifice discharge coefficient may be applied to this type of nozzle as

$$C_o = \frac{Q}{\pi r_o^2 \sqrt{2 p_i/\rho}} \tag{16}$$

Substituting for Q from equation 12:

$$C_o = \frac{A_s(1-\eta^2)}{\sqrt{A_s^2 + 4\pi^2 r_o^2 r_s^2 (1-\eta)^2}} = \frac{1-\eta^2}{\sqrt{1 + 4(1-\eta)^2 / (A_s/\pi r_o r_s)^2}} \tag{17}$$

A combination of equations 15 and 17 will permit prediction of the discharge coefficient from the nozzle constant, and equation 16 permits measurement from experimental data. Figure 8 shows a comparison of the coefficients determined by both methods for five nozzles. Figure 8 also includes values of the discharge coefficients taken from predictions published by Tanasawa and Kobayasi (3).

Cone Angle

Figure 1 shows the half-cone angle ($\alpha/2$). This cone angle may be defined as

$$\alpha = \tan^{-1}\left[\frac{(u_r)_o}{(u_a)_o}\right] \tag{18}$$

or

$$\alpha = \tan^{-1}\left[\int_{r_o}^{r_t} 2\pi\rho (u_r)_r (u_a)_r \, r\, dr \Big/ \int_{r_o}^{r_t} 2\pi\rho (u_a)_r^2 \, r\, dr\right] \tag{19}$$

or

$$\alpha = \cos^{-1}\left[\frac{(u_a)_o}{V_o}\right] \tag{20}$$

or

$$\alpha = \tan^{-1}\left[\frac{(u_r)_{r_o}}{(u_a)_{r_o}}\right] \tag{21}$$

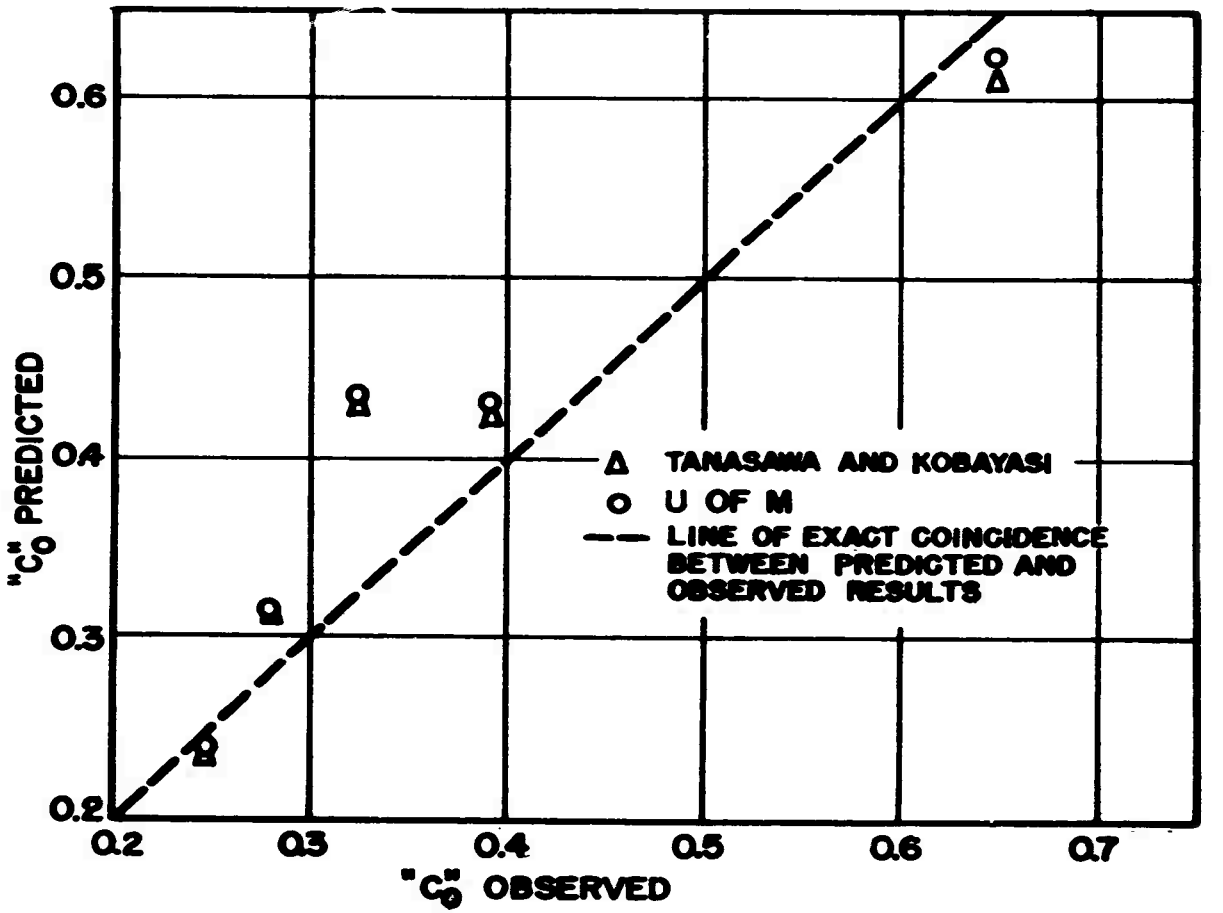

Figure 8. Comparison of Predicted and Observed Discharge Coefficients.

Equation 18 uses a ratio of mean tangential and axial velocities at the orifice, as defined by equations 8 and 9. Equation 19 is based on a ratio of tangential and axial momentums, each integrated for point functions of $(u_r)_r$ and $(u_a)_r$ along the radius from r_f to r_o. Equation 20 was proposed by G. I. Taylor (4). Equation 21 was proposed by Tanasawa and Kobayasi, relying on the value of the point functions of the velocity components taken at $r = r_o$.

These four equations are shown in Figure 9 with the half-cone angle as a function of the nozzle constant. Equation 20 was modified by using Figure 2 to convert from Taylor's term corresponding to η to the nozzle constant. Taylor's values were determined for a long orifice with a long taper in the swirl chamber, but the other three curves were for sharp-edged orifices. Four experimentally determined cone angles are also included.

Conclusions

The equations based on the assumption of potential flow seem to be verified rather well by experimental data, therefore the assumption seems justified for liquids of low viscosity at moderate velocities.

The nozzle constant, $(A_s/\pi r_o A_s)$, appears to be quite significant in controlling the various properties of the liquid sheet emerging from the nozzle. This critical factor was developed also by other authors, Tanasawa and Kobayasi (3), Vörös (5), Hinze (6), Novikov (7), and Laster and Doumas (8), and many of the predictions are checked by their work.

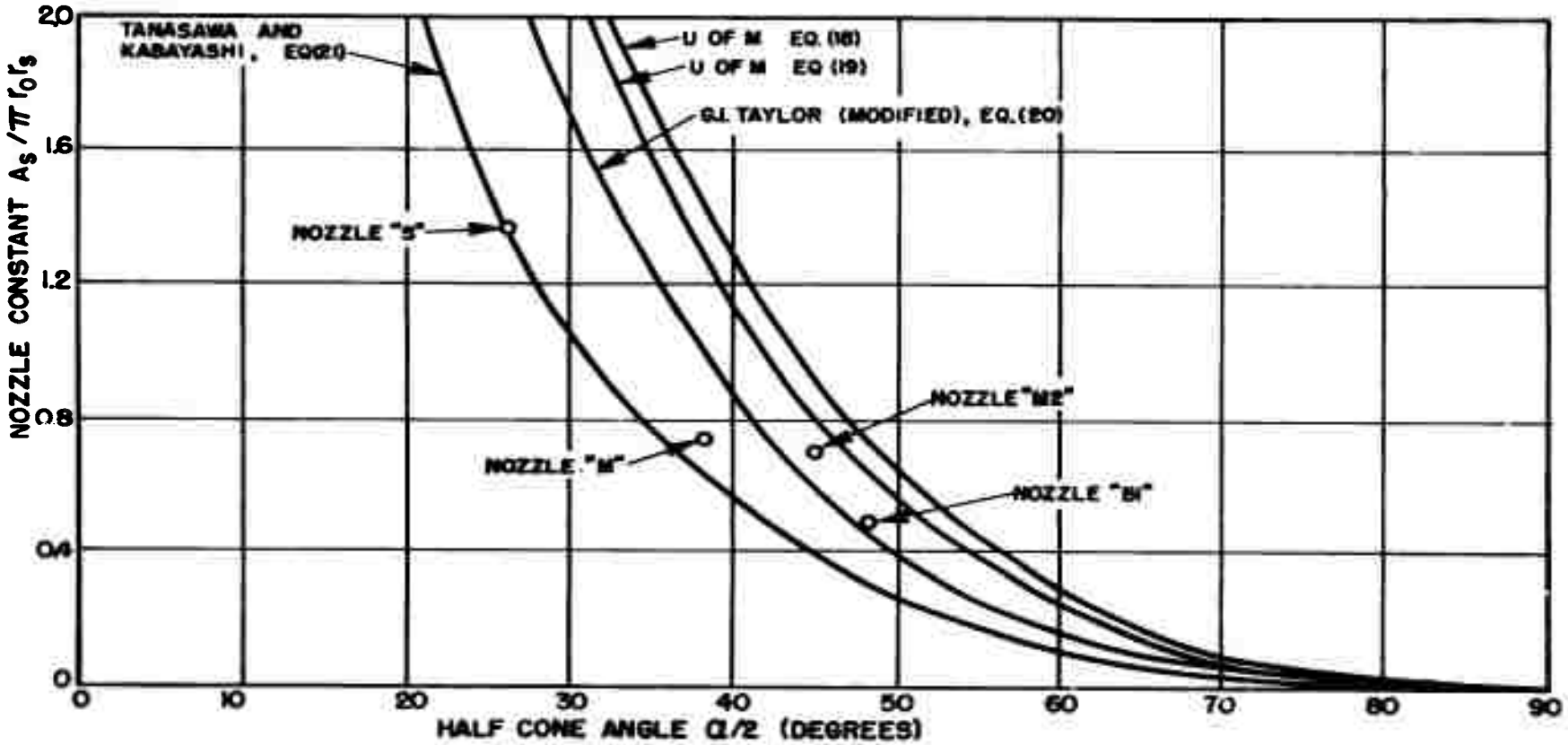

Figure 9. Effect of Nozzle Constant on Cone Angle

LITERATURE CITATIONS

1. "The Mechanism of Disintegration of Liquid Sheets," J. Louis York, H. E. Stubbs, M. R. Tek, paper 53-S-40 presented before Amer. Soc. Mech. Engrs., Columbus, Ohio, April 30, 1953.

2. "Hydrodynamica Argentorati," D. Bernoulli, 1740.

3. "Design of Swirl Nozzle by Potential Theory," Yasusi Tanasawa and Kiyosi Kobayasi (1951) (Publication unknown, reprint supplied by author).

4. "The Mechanics of Swirl Atomizers," G. I. Taylor, Proc. 7th Int. Cong. for Applied Mechanics, 1948, pp. 280-285.

5. "A cirkuláció és a kapilláris erők szerepe a cseppképzésben permetező szórófejeknél (The influence of circulation and of capillary forces in the formation of sprays in spray nozzles)," Imre Vörös, Doctor's dissertation, Royal Hungarian Univ. of Engr. (1935). Published by Springer Press, Budapest.

6. Private communication, J. O. Hinze, Royal Dutch Shell Co., Delft, Netherlands.

7. I. I. Novikov, J. of Tech. Physics (Russia), vol. 18, no. 3, 1948, pp. 345-354.

8. "Liquid Film Properties for Centrifugal Spray Nozzles," R. Laster and M. Doumas, paper presented before Am. Inst. Chemical Engrs., Cleveland, Ohio, Dec. 10, 1952.